

## A Transient N-terminal Interaction of SNAP-25 and Syntaxin Nucleates SNARE Assembly\*

Received for publication, November 4, 2003, and in revised form, December 8, 2003  
Published, JBC Papers in Press, December 9, 2003, DOI 10.1074/jbc.M312064200

Dirk Fasshauer‡ and Martin Margittai§

From the Department of Neurobiology, Max-Planck-Institute for Biophysical Chemistry, Am Fassberg 11,  
37077 Göttingen, Germany

The SNARE proteins syntaxin, SNAP-25, and synaptobrevin play a central role during  $Ca^{2+}$ -dependent exocytosis at the nerve terminal. Whereas syntaxin and SNAP-25 are located in the plasma membrane, synaptobrevin resides in the membrane of synaptic vesicles. It is thought that gradual assembly of these proteins into a membrane-bridging ternary SNARE complex ultimately leads to membrane fusion. According to this model, syntaxin and SNAP-25 constitute an acceptor complex for synaptobrevin. *In vitro*, however, syntaxin and SNAP-25 form a stable complex that contains two syntaxin molecules, one of which is occupying and possibly obstructing the binding site of synaptobrevin. To elucidate the assembly pathway of the synaptic SNAREs, we have now applied a combination of fluorescence and CD spectroscopy. We found that SNARE assembly begins with the slow and rate-limiting interaction of syntaxin and SNAP-25. Their interaction was prevented by N-terminal but not by C-terminal truncations, suggesting that for productive assembly all three participating helices must come together simultaneously. This suggests a complicated nucleation process that might be the reason for the observed slow assembly rate. N-terminal truncations of SNAP-25 and syntaxin also prevented the formation of the ternary complex, whereas neither N- nor C-terminal shortened synaptobrevin helices lost their ability to interact. This suggests that binding of synaptobrevin occurs after the establishment of the syntaxin-SNAP-25 interaction. Moreover, binding of synaptobrevin was inhibited by an excess of syntaxin, suggesting that a 1:1 interaction of syntaxin and SNAP-25 serves as the on-pathway SNARE assembly intermediate.

Following a  $Ca^{2+}$  influx into the synaptic terminal, neurotransmitter is rapidly released from synaptic vesicles that fuse with the plasma membrane. The synaptic vesicle protein synaptobrevin 2 (also referred to as vesicle-associated membrane protein 2, or VAMP 2) and the plasma membrane proteins syntaxin 1a and SNAP-25<sup>1</sup> play a central role during this

process. They belong to the family of so-called soluble N-ethylmaleimide-sensitive factor attachment protein receptor (SNARE) proteins, which are essential for all vesicular trafficking steps. It is believed that SNAREs generally initiate the process of membrane fusion by the sequential formation of a stable heteromeric “trans” complex between the vesicular and the target membranes. This basic SNARE machinery is thought to be tightly controlled by a complex protein network (for a review, see Refs. 1–5).

Syntaxin and synaptobrevin each contain a single SNARE complex-forming coiled-coil region, termed the SNARE motif, directly adjacent to their C-terminal transmembrane domain. Syntaxin 1a contains an additional regulatory N-terminal region, called the Habc domain. SNAP-25 is composed of two SNARE motifs connected by a long linker and is attached to the membrane by palmitoyl modifications in this region. Upon SNARE complex formation, major conformational changes occur, with mostly unstructured proteins forming a stable  $\alpha$ -helical complex (6–10). The mechanical force of assembly could potentially be used to overcome the repulsive forces between membranes (7). The assembled core complex consists of an elongated four-helix bundle with synaptobrevin and syntaxin each contributing one helix and SNAP-25 contributing two helices (11). In the interior, 16 layers of mostly hydrophobic amino acids are formed; however, an unusual hydrophilic layer of three glutamine residues and one arginine residue is located in the center of the bundle. Each helix can be assigned to a different SNARE subfamily. Accordingly, the SNARE helices contributing a glutamine to the zero-layer are named  $Q_a$ - (syntaxin),  $Q_b$ - (first half of SNAP-25; SN1), and  $Q_c$ -SNARE (second half of SNAP-25; SN2), whereas synaptobrevin is the R-SNARE (12, 13). A very similar structure was found in the late endosomal SNARE complex, which is only distantly related to the synaptic complex (14). In both complexes, the SNARE helices are aligned in parallel, suggesting that assembly between vesicle and target membrane originates at the membrane-distal N-terminal ends of the respective SNARE motifs and proceeds in a zipper-like fashion toward the membrane anchors (15, 16). That SNARE proteins indeed constitute a minimal membrane fusion machinery was inferred from experiments in which SNAREs were shown to slowly catalyze fusion between liposomes (17).

Since the two Q-SNAREs syntaxin and SNAP-25 mainly reside in the plasma membrane, they are presumed to cooperate in providing the binding site for the vesicular R-SNARE synaptobrevin. This concept was substantiated by the fact that both Q-SNAREs form a stable complex *in vitro*. A closer inspection of the syntaxin-SNAP-25 complex, however, revealed that it already consists of a similar four-helix bundle, in which the

saline; Syb, synaptobrevin 2; BONT/A and BONT/E, botulinum neurotoxin A and E, respectively; Syx, syntaxin.

\* The costs of publication of this article were defrayed in part by the payment of page charges. This article must therefore be hereby marked “advertisement” in accordance with 18 U.S.C. Section 1734 solely to indicate this fact.

‡ To whom correspondence should be addressed. Tel.: 49-551-201-1658; Fax: 49-551-201-1499; E-mail: dfassha@mpibpc.gwdg.de.

§ Present address: Dept. of Biochemistry and Molecular Biology, Zilkha Neurogenetic Institute, University of Southern California, Los Angeles, CA 90089.

<sup>1</sup> The abbreviations used are: SNAP-25, soluble N-ethylmaleimide-sensitive factor attachment protein of 25 kDa; SNARE, N-ethylmaleimide-sensitive factor attachment protein receptor; FRET, fluorescence resonance energy transfer; OG, Oregon Green; TR, Texas Red; IAANS, anilino-naphthalenesulfonate iodoacetamide; PBS, phosphate-buffered

binding site for synaptobrevin is taken by a second syntaxin molecule (7, 10, 18, 19). Although one cannot exclude the possibility that the second syntaxin is necessary to stabilize the Q-SNARE interaction, it seems likely that a 1:1 syntaxin-SNAP-25 interaction would provide a more straightforward synaptobrevin binding site *in vivo*. The latter scenario is corroborated by studies on a homologous Q-SNARE complex involved in exocytosis in yeast, for which a 1:1 interaction of Sso (syntaxin homologue) and Sec9p (SNAP-25 homologue) is believed to provide the binding site for Sncp (synaptobrevin homologue) (20–22).

The core region of the yeast Q-SNARE complex assembles with a relatively slow rate of  $\sim 6000 \text{ M}^{-1} \text{ s}^{-1}$  (21). This rate of Q-SNARE assembly was found to be rate-limiting for the assembly of the ternary complex. Assembly of the synaptic SNAREs is similarly slow. Furthermore, the two synaptic Q-SNAREs syntaxin and SNAP-25 have to interact to allow for subsequent synaptobrevin binding (23). These slow SNARE assembly rates probably allow for a tight control of complex formation *in vivo*, but to catalyze fast membrane fusion the reaction obviously needs accelerating factors.

Strikingly, there are no obvious obstacles such as proline residues or disulfide bonds in the relatively simple four-helix bundle structure that could account for the slow assembly rates. Nevertheless, experiments at elevated temperatures revealed that assembly could not take place in the harsh conditions in which the complex falls apart (23). It seems possible that this marked hysteresis is caused by a rather delicate nucleation reaction, which might render SNARE assembly slow. But what is the structural reason for the delicacy of SNARE nucleation? An answer to this question requires deeper insights into the molecular mechanisms of synaptic SNARE assembly. Therefore, we now have designed fluorescence assays to follow the assembly steps of the core four-helix bundle of the synaptic SNARE complex. Our results suggest that a 1:1 interaction of the Q-SNARE proteins syntaxin and SNAP-25 precedes binding of synaptobrevin. The assembly of the Q-SNAREs is rather complex, since it requires the precise N-terminal nucleation of three helices.

#### MATERIALS AND METHODS

**Protein Constructs**—The basic SNARE expression constructs, cysteine-free SNAP-25A (residues 1–206) (27), the first helix of SNAP-25A (SN1; residues 1–83), the second helix of SNAP-25A (SN2; residues 120–206), the syntaxin 1A SNARE motif (SyxH3; residues 180–262), and synaptobrevin 2 (Syb; residues 1–96) (8) have been described before. Shortened versions of these constructs were cloned into the pET28a vector. The following shortened constructs were generated: SNAP-25A, BoNT/A fragment (residues 1–197), SN25ΔC (residues 1–180), ΔNSN25 (residues 39–206), SN1short (residues 7–83), ΔNSN1 (residues 39–83), SN1ΔC (residues 7–66), SN2short (residues 141–204), ΔNSN2 (residues 159–206), and SN1ΔC (residues 141–188); SyxH3, ΔNSyxB3 (residues 212–262) and SyxB3ΔC (residues 183–240); Syb, Syb 1–81 (residues 1–81), SybΔC (residues 1–70), and ΔNSyB (residues 42–96).

In addition, we utilized a variety of single cysteine variants of all three SNARE proteins that had been previously characterized by EPR spectroscopy (10). The following single cysteine variants of SyxB3 (residues 183–262) were used: Cys<sup>225</sup>, Cys<sup>240</sup>, and Cys<sup>248</sup>. Synaptobrevin 2 (residues 1–96) Cys<sup>79</sup> and full-length SNAP-25A Cys<sup>34</sup> were also used.

**Protein Purification**—The different synaptic SNARE protein fragments were isolated from *E. coli* and purified by Ni<sup>2+</sup>-nitrilotriacetic acid affinity chromatography followed by ion exchange chromatography on an Äkta system (Amersham Biosciences) essentially as described (8, 27). The purity was greater than 95% as determined by SDS-PAGE. All ternary SNARE complexes were assembled overnight from purified individual proteins and purified using a Mono Q-column. Protein concentration was determined by absorption at 280 nm in the presence of guanidine HCl or for the individual SNAP-25 helices and the C-terminally truncated synaptobrevin constructs, which do not possess aromatic residues, using the Bradford assay.

**Labeling**—The sulfhydryl-reactive fluorescent probes anilino-naphthalenesulfonate iodoacetamide (IAANS) Oregon Green 488 iodoacetamide and Texas Red C5 bromoacetamide were purchased from Molecular Probes, Inc. (Eugene, OR). Before labeling, SNARE proteins ( $\sim 1\text{--}4 \text{ mg/ml}$ ) containing a single cysteine were dialyzed against degassed PBS buffer (20 mM sodium phosphate, pH 7.4, 100 mM NaCl). About a 10–20-fold molar excess of the respective fluorescence probe in *N,N*-dimethylformamide was added and incubated for 2 h. The reaction was stopped by adding 10 mM dithiothreitol. After 1 h, excess dye was removed by gel filtration on a Sephadex G-50 column. Afterward, the labeled protein was dialyzed against PBS buffer. The concentration of the labeled protein was determined from its absorption at 327 nm (IAANS), 488 nm (Oregon Green), or 595 nm (Texas Red) using the molar extinction coefficients of the dyes. The protein concentration was determined by the Bradford assay.

**Fluorescence Spectroscopy**—All measurements were carried out in a Fluoromax 2 spectrometer equipped with autopolarizers (Jobin Yvon) in PBS buffer at 25 °C in 1-cm quartz cuvettes.

For measurements of IAANS-labeled molecules, the excitation wavelength was 327 nm, and the emission spectrum was measured from 370 to 600 nm. The slit width of the excitation light was set at 2 nm, and that of the emission was set from 2.5 to 4 nm. Initially, the spectrum of the labeled molecule was measured and compared with the spectrum after the addition of unlabeled, interacting protein(s). Kinetic measurements were then performed using the emission wavelength at which the maximum change had been observed.

Changes of anisotropy upon complex formation using proteins labeled with Oregon Green were measured at an excitation wavelength of 488 nm and an emission wavelength of 520 nm. The slit widths were set to 2–4 nm, and the integration time was set at 1 s. At first, the *G* factor was determined according to  $G = I_{\text{HV}}/I_{\text{HH}}$ , where *I* is the fluorescence intensity, and the first subscript letter indicates the direction of the exciting light and second subscript letter is the direction of emitted light. Then the intensities of the vertically and horizontally polarized emission light after excitation by vertically polarized light were measured. The anisotropy (*r*) was calculated automatically according to  $r = (I_{\text{VV}} - G \times I_{\text{VH}})/(I_{\text{VV}} + 2 \times G \times I_{\text{VH}})$ . At the beginning of the reaction, data points were recorded using the smallest interval possible ( $\sim 5 \text{ s}$ ). Later, the intervals were extended accordingly.

For fluorescence resonance energy transfer (FRET) measurements, the emission spectrum was recorded from 500 to 700 nm at an excitation of 488 nm. For kinetic measurements, the change of the fluorescence intensity of the acceptor was recorded.

**CD Spectroscopy**—CD measurements were performed using a Jasco model J-720 instrument. For spectral measurements, different protein combinations at a concentration of about 5–10 μM in 20 mM Tris, pH 7.4, 100 mM NaCl (for details, see the appropriate figure legend) were incubated overnight. Hellma quartz cuvettes with a path length of 0.1 cm were used. The spectra were obtained by averaging over 5–50 scans using steps of 0.2 nm with a scan rate of 50 nm/min essentially as described (8, 27). The measurements were carried out at 25 °C.

Kinetic measurements were carried out in PBS buffer using 1-cm quartz cuvettes at 25 °C. Proteins were mixed, and the change in the CD signal was followed at 220 nm.

For thermal denaturation experiments, the purified ternary SNARE complexes were dialyzed against PBS buffer. The ellipticity at 220 nm was recorded between 25 and 95 °C at a temperature increment of 30 °C/h.

#### RESULTS

During SNARE assembly, major structural rearrangements occur, with mostly unstructured monomers forming complexes with high  $\alpha$ -helical content. This allows us to monitor the assembly reaction using CD spectroscopy (6, 7, 23). This approach alone, however, does not provide the spatial information necessary for a detailed analysis of the assembly pathway, since intermediate products already exhibit similar changes in the secondary structure (8). To overcome these shortcomings, we have now introduced fluorescence probes into each of the three SNARE complex constituents. Using the crystal structure (11) as a guide, several positions in each SNARE protein were chosen for fluorescence labeling. Throughout the study, only the soluble regions of the three synaptic SNAREs that form the core complex were used. An overview of the different labeling positions is given in Fig. 1.

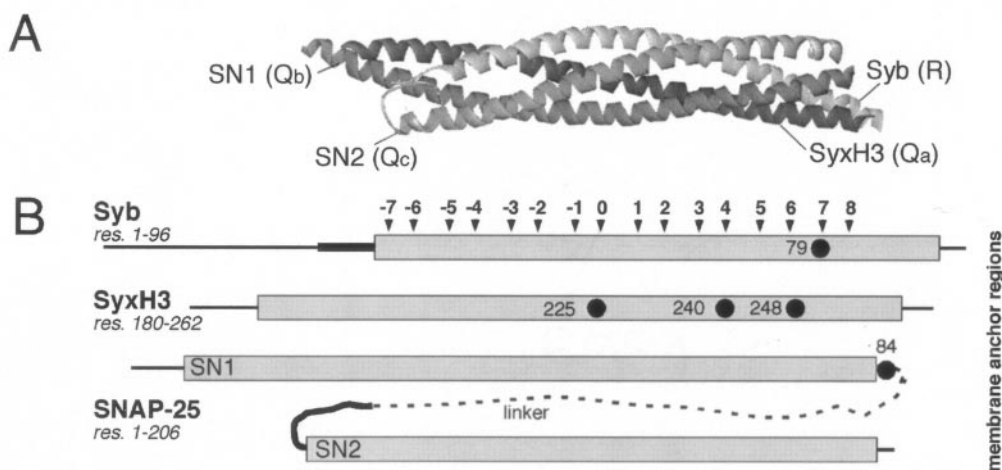


FIG. 1. **Schematic representation of the structure of the core synaptic SNARE complex.** *A*, ribbon diagram of the parallel four-helix bundle structure of the synaptic SNARE complex (11), to which Syb (R helix) and Syx (Q<sub>a</sub> helix) each contribute one helix and SNAP-25 contributes two helices (SN1, Q<sub>b</sub> helix; SN2, Q<sub>c</sub> helix). *B*, schematic representation of the SNARE constructs used. The helical regions of the four-helix bundle are boxed, and additional structured regions are indicated by thick lines. The interacting coiled-coil layers, numbered from -7 to +8, are indicated by the arrowheads on top. Single cysteines used for fluorescence labeling are specified by black circles and residue number.

*A Second Syntaxin Competes with Synaptobrevin for Binding to a 1:1 SyxH3-SNAP-25 Intermediate*—In our experiment, we mainly utilized the fluorophore IAANS, which exhibits environmentally sensitive fluorescence properties. Only a few positions of those tested exhibited a pronounced change in the fluorescence intensity that allowed us to follow SNARE assembly. As an example, SNAP-25 labeled at position 84 (SNAP-25<sup>84IAANS</sup>) showed a strong increase in fluorescence intensity upon binding to syntaxin (Fig. 2*B*). At pseudo-first-order conditions, the rate of assembly was  $\sim 6000 \text{ M}^{-1} \text{ s}^{-1}$  (Fig. 2*D*). Comparable rates were obtained when the SNARE motif of syntaxin (SyxH3) was labeled with IAANS at position 225, 240, or 248 and mixed with SNAP-25 ( $\sim 7600$ ,  $\sim 6800$ , and  $\sim 7400 \text{ M}^{-1} \text{ s}^{-1}$ , respectively) (Fig. 2*C*). Upon titration, saturation of fluorescence was reached at a molar ratio of about two SyxH3 and one SNAP-25 molecule, whereas in the presence of Syb, a molar ratio of 1:1 between SyxH3 and SNAP-25 was observed (data not shown). However, in all experiments in which the reaction between SyxH3 and SNAP-25 was monitored, no clear indication for a two-step assembly process was observable. A possible explanation might be that a transient 1:1 intermediate of SyxH3 and SNAP-25 creates a new binding site with increased affinity for the second SyxH3.

In the presence of Syb, the entire reaction appeared to be slower (Fig. 2, *A* and *B*) and to consist of at least two phases as we had previously observed using CD spectroscopy (23). As a different read-out for ternary complex formation, we then used Syb labeled at position 79 (Syb<sup>79IAANS</sup>), which exhibited a clear rise in fluorescence intensity only upon the addition of both SyxH3 and SNAP-25. Interestingly, complex formation was faster when increasing amounts of SNAP-25 were added and SyxH3 was kept at a constant concentration (Fig. 3*A*), whereas increasing amounts of SyxH3 rather slowed down assembly (Fig. 3*B*). Thus, it appears that an excess of SyxH3 inhibits Syb binding, most likely because both molecules compete for the same binding site offered by a transient 1:1 SyxH3-SN25 intermediate. Nevertheless, ternary complex formation was only slightly faster when SyxH3 and SNAP-25 were allowed to assemble beforehand (data not shown). This accelerating effect was most obvious when more SNAP-25 than SyxH3 was used. This probably suggests that only a small portion of premixed Q-SNAREs reside as transient 1:1 complexes, whereas the majority appears to exist as stable 2:1 complexes, which do not appear to serve as the primary binding site for synaptobrevin.

In another set of experiments, we added SNAP-25 to a mix of SyxH3<sup>225OG</sup> and SyxH3<sup>225TR</sup> (*i.e.* syntaxins labeled at position 225 with the fluorescence dyes Oregon Green or Texas Red, respectively). Although this approach allowed only for a random integration of the differently labeled syntaxins, assembly gave rise to clear FRET, confirming that the Q-SNARE assembly contained two syntaxin molecules (Fig. 4, *inset*). At pseudo-first-order conditions, a Q-SNARE assembly rate of  $\sim 5900 \text{ M}^{-1} \text{ s}^{-1}$  was observed (data not shown), which is similar to the ones assessed with IAANS-labeled Q-SNAREs (see above). Upon the addition of an excess of Syb to the preassembled Q-SNARE complex, the FRET signal disappeared (Fig. 4), suggesting that one of the syntaxin molecules of the preformed 2:1 complex had been exchanged for Syb. The addition of an excess of unlabeled SyxH3 to the preformed Q-SNARE complex led to a comparable disappearance of the FRET signal (Fig. 4), which probably reflects the dissociation of the second syntaxin. Since Syb binding was not faster than the off-rate of the second syntaxin, it is likely that Syb does not actively replace one of the two syntaxins from the 2:1 Q-SNARE assembly.

*The Syntaxin-SNAP-25 Interaction Nucleates N-terminal-ly*—To assess which regions of the SNAREs are sufficient for assembly, N- or C-terminal parts of the SNARE motifs were removed (see Fig. 1). Remarkably, N-terminally truncated SNAP-25 (residues 39–206;  $\Delta$ NSN25) as well as N-terminally truncated SyxH3 (residues 212–262;  $\Delta$ NSyxH3) appeared to have lost their ability to undergo Q-SNARE interaction (Fig. 5, *A* and *B*). A similar result was obtained by CD spectroscopy, where no increase in  $\alpha$ -helical content was observed for a mix of each of the constructs with the respective intact Q-SNARE binding partner (Fig. 5*C*). Furthermore, these constructs almost completely lost their ability to form a ternary complex containing Syb; only at high concentrations ( $> 5 \mu\text{M}$ ), a stable ternary complex slowly formed ( $> 24 \text{ h}$ ) (Fig. 5*C*). This indicates that when the Q-SNARE interaction is perturbed, assembly occurs slowly due to a high energy barrier.

In contrast, a C-terminally truncated SyxH3 (residues 183–240; SyxH3 $\Delta$ C) was still able to interact with SNAP-25 (Fig. 5*A*). Likewise, a C-terminally truncated SNAP-25 (residues 1–197), which resembles the botulinum neurotoxin A (BoNT/A) cleavage product, formed a complex with SyxH3 (data not shown). However, further shortened SNAP-25 construct (residues 1–180; SN25 $\Delta$ C, which resembles the BoNT/E cleavage product) only slowly interacted with SyxH3 (Fig. 5*B*). Never-

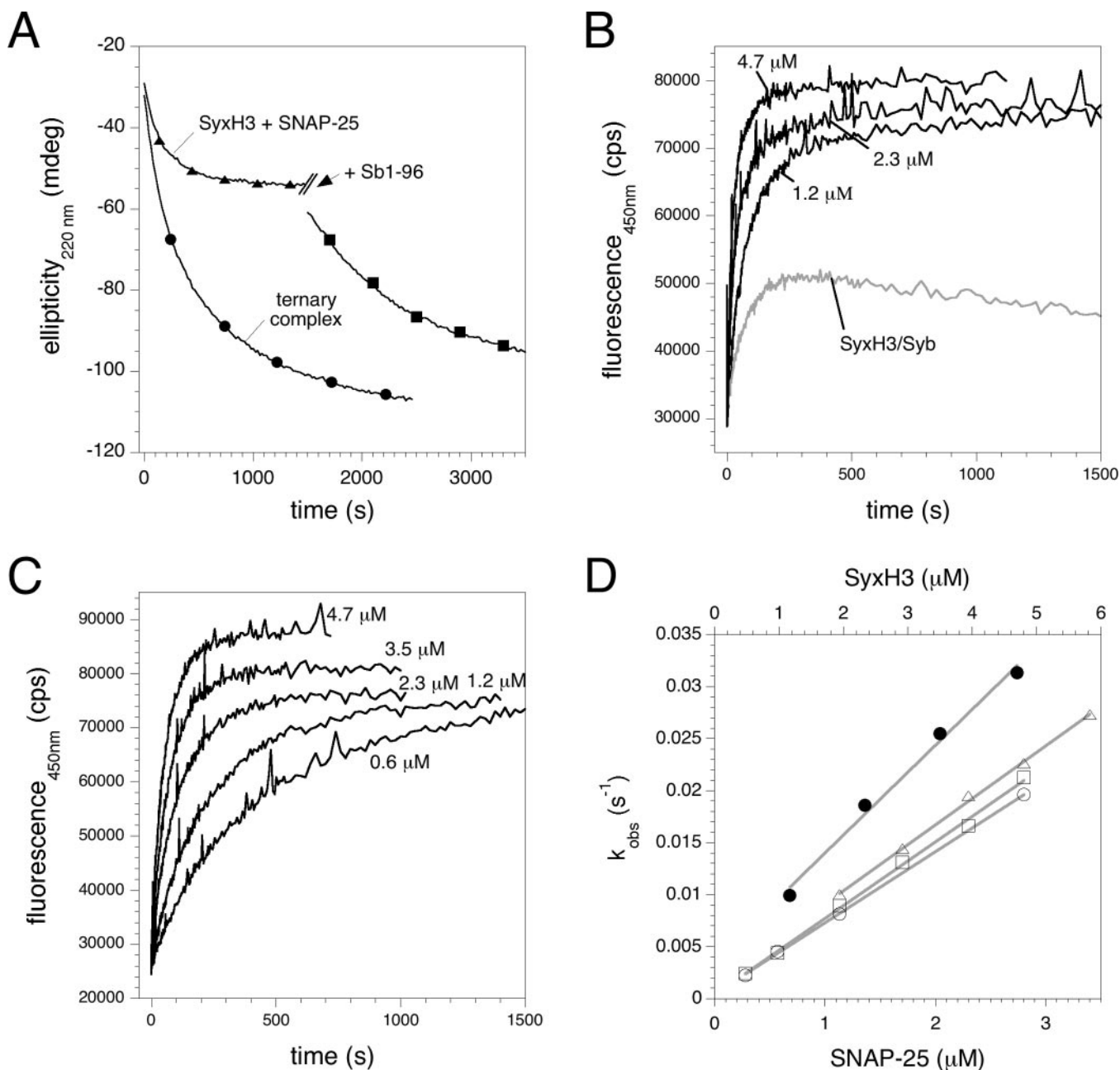


**FIG. 2. Slow formation of the syntaxin-SNAP-25 complex.** *A*, SNARE assembly was monitored by CD spectroscopy at 220 nm over time. Proteins were mixed at a concentration of 1.5  $\mu\text{M}$  each. ●, formation of the ternary core SNARE complex; ▲, assembly of SyxH3 and SNAP-25. Syb was added as indicated after assembly of SyxH3 and SNAP-25 (■). Note that the increase in  $\alpha$ -helical content upon mixing SyxH3 and SNAP-25 was less pronounced, since both proteins were mixed in a 1:1 molar ratio, whereas a more pronounced increase was observed at a 2:1 ratio (data not shown). *B*, SNAP-25 labeled with IAANS at position 84 (SNAP-25<sup>84IAANS</sup>, ~200 nM) was mixed with the indicated amounts of SyxH3 alone (black lines) or SyxH3 premixed with Syb (both 1.2  $\mu\text{M}$ ; gray line). The change in the fluorescence at 450 nm was monitored over time. Similar results were obtained when SyxH3 and Syb were unfolded in guanidine hydrochloride (final concentration <100 mM; data not shown). *C*, SyxH3<sup>248IAANS</sup> (~200 nM) was mixed with the indicated amounts of SNAP-25. *D*, the pseudo-first-order rate constants obtained from the single exponential fits of the reaction of SNAP-25<sup>84IAANS</sup> with increasing amounts of SyxH3 were plotted against the concentration of SyxH3 (●, upper *x* axis). Likewise, the pseudo-first-order rate constants of the reactions of SyxH3<sup>225IAANS</sup> (▲), SyxH3<sup>240IAANS</sup> (○), and SyxH3<sup>248IAANS</sup> (□) with different amounts of SNAP-25 were plotted as a function of the SNAP-25 concentration (lower *x*-axis). The slope of the linear fits (gray lines) yielded the second-order rate of the reaction (SNAP-25<sup>84IAANS</sup> ~6000  $\text{M}^{-1} \text{s}^{-1}$ , SyxH3<sup>225IAANS</sup> ~7600  $\text{M}^{-1} \text{s}^{-1}$ , SyxH3<sup>240IAANS</sup> ~6800  $\text{M}^{-1} \text{s}^{-1}$ , and SyxH3<sup>248IAANS</sup> ~7400  $\text{M}^{-1} \text{s}^{-1}$ ). Note that position 225 of SyxH3 is on the surface of the assembled SNARE complex, whereas positions 240 and 248 point inward.

theless, upon the addition of Syb, SN25 $\Delta$ C readily formed a ternary SNARE complex (Fig. 5B). The molecular mass of the purified SyxH3-SN25 $\Delta$ C complex determined by multiangle laser light scattering indicated a 2:2 stoichiometry (data not shown). An equivalent 2:2 complex has been described for the isolated first helix of SNAP-25 (SN1) and SyxH3 (24). Thus, in the absence of Syb, the much shortened second helix of the SN25 $\Delta$ C construct may not suffice to prevent the competing

but slow process of dimerization (for illustration, see Fig. 6). To test whether Syb truncations affected SNARE assembly, we utilized the increase in fluorescence anisotropy of SyxH3<sup>225OG</sup> upon complex formation. Upon assembly with SNAP-25, anisotropy of SyxH3<sup>225OG</sup> exhibited only a small increase, which might be caused by the proximity of two OG fluorophores in the SyxH3<sub>2</sub>-SNAP-25<sub>1</sub> complex. A much more pronounced rise, however, was observed upon ternary SNARE complex forma-

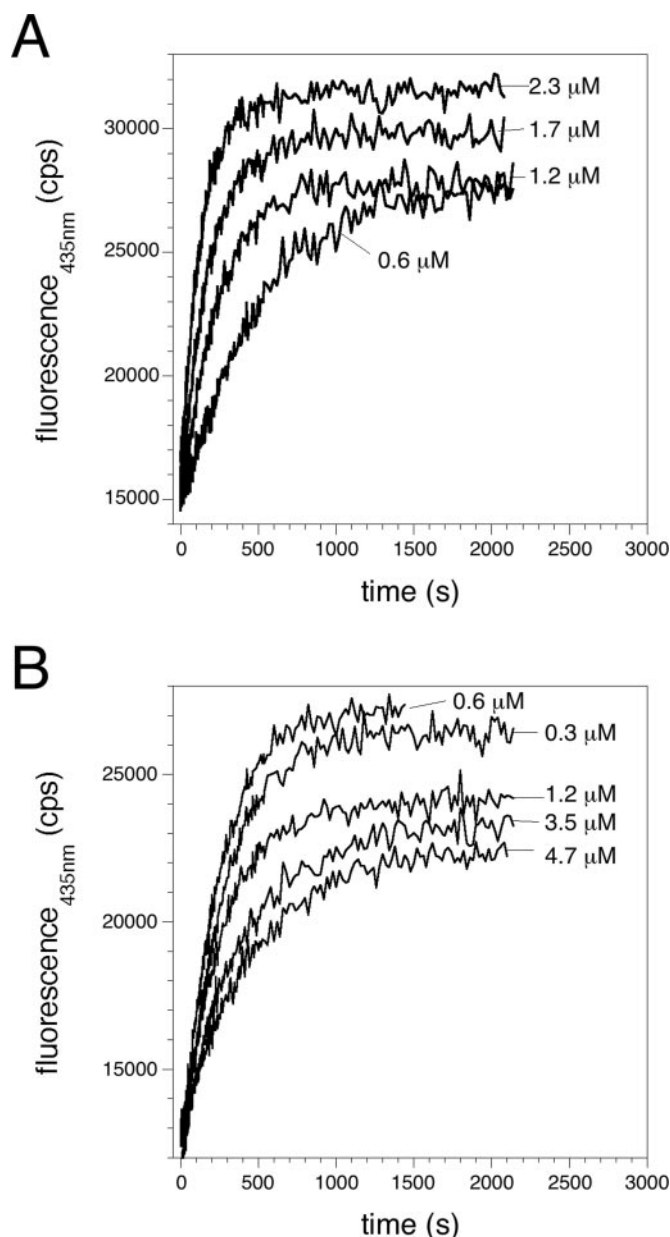


FIG. 3. **Syntaxin competes with synaptobrevin for binding to a 1:1 Q-SNARE intermediate.** The fluorescence change at 435 nm of Syb<sup>79IAANS</sup> (~200 nM) was monitored upon mixing with 230 nM SyxH3 and the indicated amounts of SNAP-25 (A) or upon mixing with 1.2  $\mu$ M SNAP-25 and the indicated amounts of SyxH3 (B).

tion. Interestingly, N- or C-terminal truncations of Syb had no significant effect on SNARE assembly (Fig. 5D). Similar results were obtained by CD spectroscopy (Fig. 5C). Taken together, these results substantiate the view that Syb binding occurs after Q-SNARE nucleation.

Although all of the above SNARE truncations removed a substantial part of the core complex-forming region, about three hydrophobic coiled-coil layers (see Fig. 1), their core complexes remained highly stable (Table I). Consequently, the pronounced effect of the truncations on assembly cannot simply be explained by the fact that the resulting core complex is less stable. Rather, the stability of the Q-SNARE intermediate is likely to be mostly affected. The SNARE complex containing  $\Delta$ NSyH3 did not refold during the time period tested, confirming our results that assembly of this fragment is extremely slow (data not shown). Remarkably, complexes containing either N- or C-terminally truncated Syb still exhibited a strong hystere-

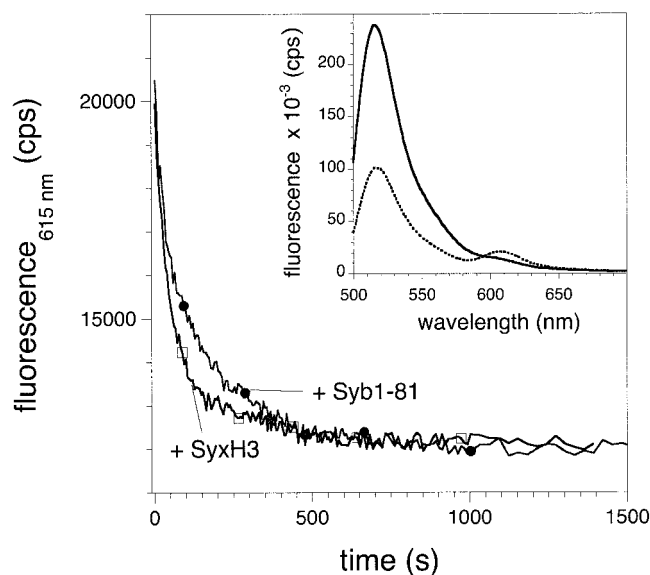
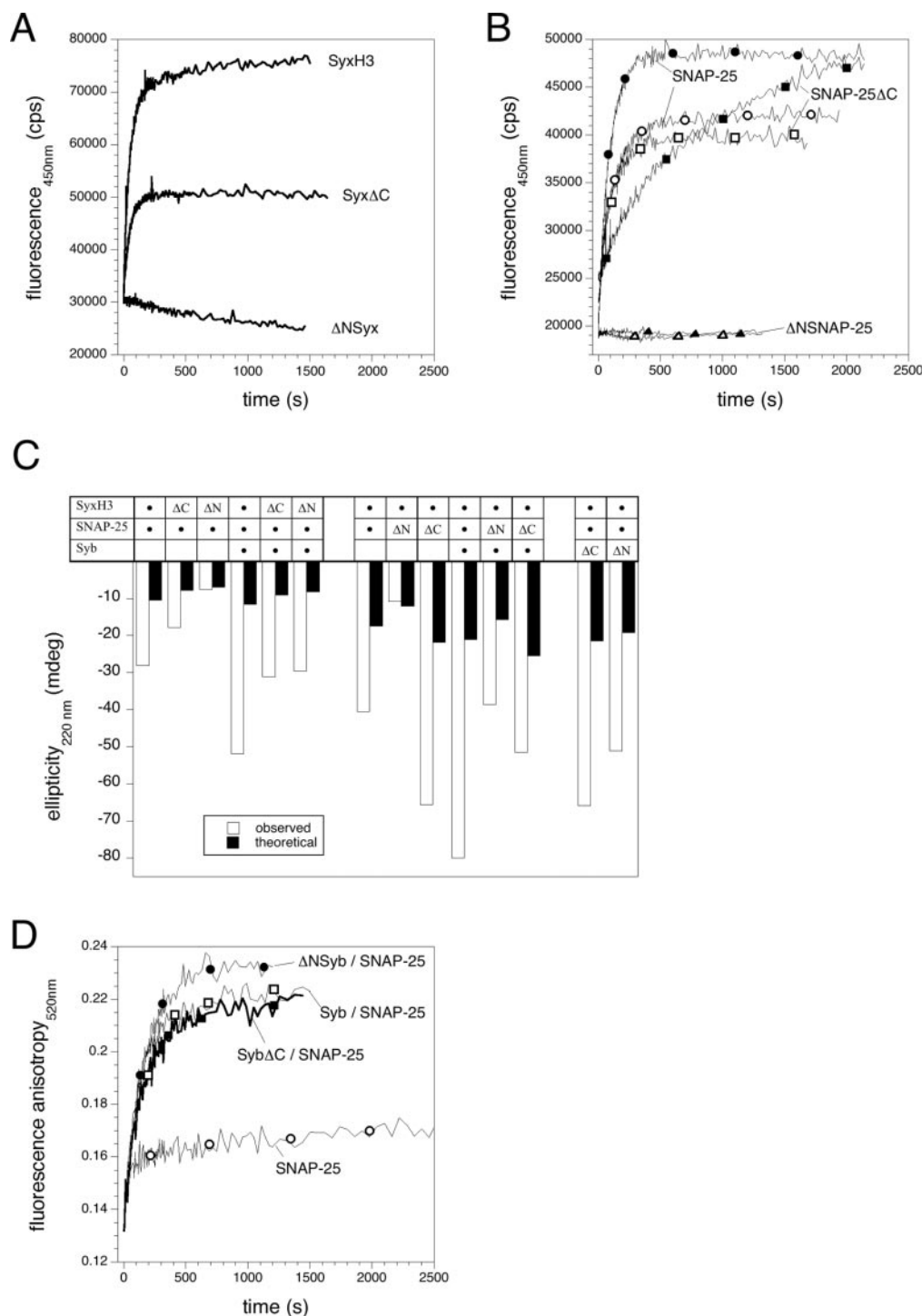


FIG. 4. **Dissociation of the second syntaxin from the 2:1 Q-SNARE complex is a prerequisite for synaptobrevin binding.** Upon assembly of SNAP-25 (~340 nM) with two differently labeled syntaxins (labeled with Oregon Green, SyxH3<sup>225OG</sup>, or Texas Red, SyxH3<sup>225TR</sup>, each at ~200 nM), a clear FRET signal upon excitation at 488 nm was detected (inset, black line). For kinetic measurements, the change of the acceptor fluorescence at 615 nm was followed. Upon the addition of a large excess of unlabeled SyxH3 (~10  $\mu$ M), the FRET signal disappeared with a half-life of ~71 s.  $\square$ , the addition of a large excess of Syb 1–81 (~9  $\mu$ M) to the preassembled Q-SNAREs led to a similar, but slightly slower, disappearance of the FRET signal ( $\bullet$ , gray line). Note that in these experiments, a slightly truncated Syb construct (Syb 1–81) was used to minimize unspecific aggregation and quenching effects caused by the positively charged C-terminal residues of Syb (residues 1–96).

sis (data not shown), suggesting that fragments of the Syb helix are sufficient to produce an “irreversible” SNARE interaction.

*The Q-SNARE Helices Work Together for Nucleation*—The SNARE protein SNAP-25 contains two SNARE motifs connected by a flexible linker region (10), which spans the entire length of the SNARE bundle in the core complex. Therefore, the question arises whether both SNAP-25 helices are necessary for successful nucleation of the Q-SNARE complex. For a detailed analysis of this process, we applied the same fluorescence approaches using the two helices of SNAP-25 as independent fragments. Neither of the two individual SNAP-25 helices produced a significant increase in fluorescence intensity upon mixing with SyxH3<sup>225IAANS</sup>, whereas both helices together led to a concentration-dependent increase in fluorescence intensity (Fig. 7a). A comparable result was also obtained when SyxH3<sup>240IAANS</sup> was used (data not shown). The fluorescence intensity increase of SyxH3<sup>225IAANS</sup> depended on the presence of two labeled syntaxin molecules in close proximity, since mixing with unlabeled SyxH3 readily reduced the fluorescence increase. This suggests that in the presence of both SNAP-25 helices, a Q-SNARE complex containing two syntaxin molecules had formed. Interestingly, assembly in the presence of two independent helices of SNAP-25 was significantly slower and required much higher protein concentrations than with full-length SNAP-25, confirming previous results achieved by CD spectroscopy (24) and suggesting that both SNAP-25 helices cooperate for productive assembly.

To investigate whether truncations of the first SNAP-25 helix would change its ability to interact with syntaxin, we first used CD spectroscopy. Interestingly, in contrast to a full SN1 helix, neither an N-terminally (residues 39–83;  $\Delta$ NSN1) nor C-terminally (residues 7–67; SN1 $\Delta$ C) truncated helix dis-



**FIG. 5. N-terminal truncations in the coiled-coil region of the Q-SNAREs prevent assembly.** *A*, SNAP-25<sup>84IAANS</sup> (~200 nm) was mixed with ~2 μM N- or C-terminally truncated syntaxin SNARE motifs (ΔNSyH3, residues 212–262; SyxH3ΔC, residues 183–240, respectively). Note that the overall increase in fluorescence intensity upon binding of SyxH3ΔC (residues 183–240) was smaller than with the intact SyxH3 (residues 180–262; see also Fig. 2B), probably because fewer conformational changes extended into the C-terminal region of SNAP-25, which carried the fluorophore. *B*, the fluorescence change of SyxH3<sup>240IAANS</sup> (~200 nm) was monitored upon mixing with ~1.2 μM full-length SNAP-25 (●), N-terminally (ΔNSN25; residues 39–206) (▲), or C-terminally truncated SNAP-25 (SN25ΔC, residues 1–180) (■). Similar experiments were carried out in the presence of ~2 μM Syb 1–81 (open symbols). *C*, anisotropy of SyxH3<sup>225OG</sup> (~100 nm) was monitored after mixing with SNAP-25 alone or in the presence of Syb or N-terminally (ΔNSyb; residues 42–96) or C-terminally (SybΔC; residues 1–70) truncated synaptobrevin variants. *D*, changes in the CD signal at 220 nm of the different truncated SNARE proteins. *Black columns* denote the theoretical noninteracting signal (*i.e.* the sum of the signal of the unmixed components), whereas *white columns* represent the observed signal after overnight mixing of equimolar concentrations of the indicated protein combinations. The first six combinations were mixed at about 6 μM and all others at about 9.3 μM concentrations of the individual proteins. ΔN and ΔC indicate the above mentioned N- and C-terminally truncated SNAREs, respectively.

played a structural change upon mixing with syntaxin (data not shown). Similarly, both shortened syntaxin variants (SyxH3ΔC and ΔNSyH3) did not exhibit a structural change upon mixing with SN1 (data not shown). Whereas we had

expected, in the light of our above mentioned results, that the N-terminally truncated fragments would not be able to assemble, we had not anticipated the additional inability of the C-terminally truncated helix to assemble. One possible explana-

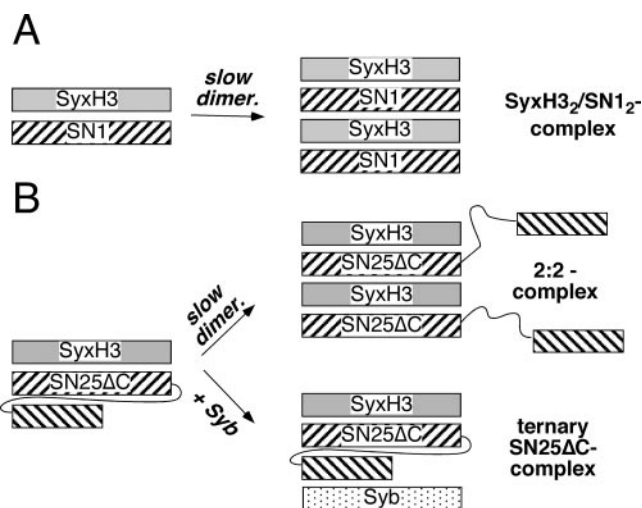


**FIG. 6. Schematic representation of the assembly pathway of a C-terminal truncated SNAP-25.** *A*, the SNARE motif of syntaxin (SyxH3) and the first helix of SNAP-25 (SN1) slowly form a stable assembly. This assembly exhibits a 2:2 stoichiometry and consists of an extended parallel four-helix bundle similar to that of the core SNARE complex (24). The SyxH3<sub>2</sub>SN1<sub>2</sub> complex probably represents an off-pathway SNARE assembly, which forms via slow dimerization of a SyxH3-SN1 intermediate. *B*, C-terminally truncated SNAP-25 (SN25ΔC) and SyxH3 assemble into a complex resembling the SyxH3<sub>2</sub>SN1<sub>2</sub> complex. Probably, the truncated SN2 helix of the SN25ΔC-construct does not prevent dimerization but is only loosely connected to the four-helix bundle. In the presence of Syb, however, SN25ΔC supports the formation of the ternary SNARE complex at the rate of full-length SNAP-25.

TABLE I

Melting temperatures of core SNARE complexes containing truncated fragments measured by CD spectroscopy

Complexes were kept in a 20 mM sodium phosphate buffer (pH 7.4) containing 100 mM NaCl.

Complexes	Temperatures
Sx 183–240	78 °C
Sx 212–262	72 °C
Sb 1–70	79 °C
Sb 42–96	72 °C
SN25ΔC	65 °C
Core synaptic SNARE complex	82 °C (23)
SyxH3 <sub>2</sub> -SNAP-25 <sub>1</sub> complex	44.5 °C at 7 μM (23)

tion for this finding is that the C-terminal regions of SN1 and of SyxH3 are necessary for dimerization into the  $\alpha$ -helical SyxH3<sub>2</sub>SN1<sub>2</sub> complex (Fig. 5). Nevertheless, the addition of SN2 to a mixture of SN1ΔC and SyxH3 led to a slow induction of  $\alpha$ -helical structure (*i.e.* Q-SNARE complex formation) (data not shown), whereas no such induction was found with the  $\Delta$ NSN1 fragment. A structural change was also observed when both individual SNAP-25 helices were mixed with SyxH3ΔC but not with  $\Delta$ NSyxB3 (data not shown). Similarly, the addition of the SN1ΔC fragment but not the  $\Delta$ NSN1 fragment to a mix of SyxH3<sup>225OG</sup> and SN2 showed a clear rise in fluorescence intensity (Fig. 7B). Taken together, this largely confirms that the N-terminal regions of the SyxH3 and SN1 are necessary for Q-SNARE assembly.

Mixing the N-terminally shortened second SNAP-25 helix (residues 159–206;  $\Delta$ NSN2) with SN1 and SyxH3<sup>225IAANS</sup> did not produce a fluorescence change (Fig. 7B), suggesting that the N-terminal portion of all three Q-SNARE helices is required for assembly. Unexpectedly, however, the C-terminally shortened second SNAP-25 helix (residues 141–188; SN2ΔC) also appeared to be incapable of supporting the formation of a Q-SNARE complex (Fig. 7B). Yet, considering our observations made with the BoNT/E-fragment of SNAP-25 (SN25ΔC; Fig.

4B), it seemed likely that SN2ΔC could, in principle, nucleate Q-SNARE assembly but, like SN25ΔC, could not prevent the competing dimerization process into the SyxH3<sub>2</sub>-SN1<sub>2</sub> complex (Fig. 6). To test whether SN2ΔC might be able to support assembly in the presence of Syb, we monitored the anisotropy of SyxH3<sup>225OG</sup>, since it primarily denotes the formation of the Syb-containing SNARE complex. The addition of both individual helices of SNAP-25 to SyxH3<sup>225OG</sup> did not produce a significant increase in anisotropy, whereas the addition of Syb produced a clear increase in anisotropy (Fig. 7C). C-terminal truncations of either one of the two SNAP-25 helices exhibited a similar increase in anisotropy, indicating that they indeed allowed SNARE assembly. In contrast, N-terminal truncations of either one of the two SNAP-25 helices abolished SNARE complex formation (Fig. 7C).

Altogether, our results suggest that assembly of SyxH3 and SNAP-25 requires the orchestrated coming together of the N-terminal portions of all three Q-SNARE helices. After successful nucleation, the free binding site is readily occupied, by a second SyxH3 or Syb molecule.

## DISCUSSION

The SNARE proteins syntaxin 1, SNAP-25, and synaptobrevin 2 are widely believed to constitute the basic catalytic machinery of the complex neurotransmitter release apparatus. It has been suggested that they gradually assemble into a tight complex between the synaptic vesicle and plasma membrane. Final zippering of this complex would lead to the fusion of the two membranes (15, 16).

Using CD spectroscopy, we have previously shown that the interaction of syntaxin and SNAP-25 serves as an essential intermediate for the assembly of the synaptic SNARE complex (23). This approach, however, did not allow us to clarify whether this intermediate consists of a four-helix bundle syntaxin<sub>2</sub>-SNAP-25<sub>1</sub> complex or an entity containing only one copy of syntaxin. To achieve a more detailed picture of the assembly steps and the involved intermediates, we have now used fluorescence spectroscopy.

We found that assembly of the SNARE motif of syntaxin (SyxH3) and SNAP-25 occurred with the relatively slow rate of  $\sim 7000 \text{ M}^{-1} \text{ s}^{-1}$ . After assembly, a majority of the proteins resided in a complex with 2:1 stoichiometry. This Syx<sub>2</sub>-SNAP-25<sub>1</sub> complex has been shown to resemble the four-helix bundle structure of the ternary SNARE complex, but with a second syntaxin molecule occupying the binding site of synaptobrevin (7, 10, 18, 19). Since we did not observe two distinct steps during the assembly of syntaxin and SNAP-25, it seems possible that the fluorescence techniques used were still not suited to detecting both binding events. Another, more likely explanation is that the first step, nucleation of a 1:1 Syx-SNAP-25 complex, is rate-limiting, concealing the faster binding of a second syntaxin molecule. Furthermore, syntaxin appeared to efficiently compete with synaptobrevin, suggesting that both molecules bind onto the same transient 1:1 intermediate. Consequently, the kinetics of ternary complex assembly were rather complex and did not allow us to directly assess the rate of synaptobrevin binding. Nevertheless, our data suggest that the transient 1:1 Syx-SNAP-25 interaction allows for fast binding of synaptobrevin. Further studies to test this possibility are in progress.

A similar assembly rate of  $\sim 6000 \text{ M}^{-1} \text{ s}^{-1}$  was observed for the interaction of the core regions of the exocytotic yeast Q-SNAREs Sso1p (syntaxin homologue) and Sec9p (SNAP-25 homologue) (21). The yeast Q-SNARE complex consists of a 1:1 heterodimer (20, 21), forming a three-helix bundle that is structured only in the N-terminal two-thirds of the three participating SNARE motifs (22). This heterodimer was suggested to

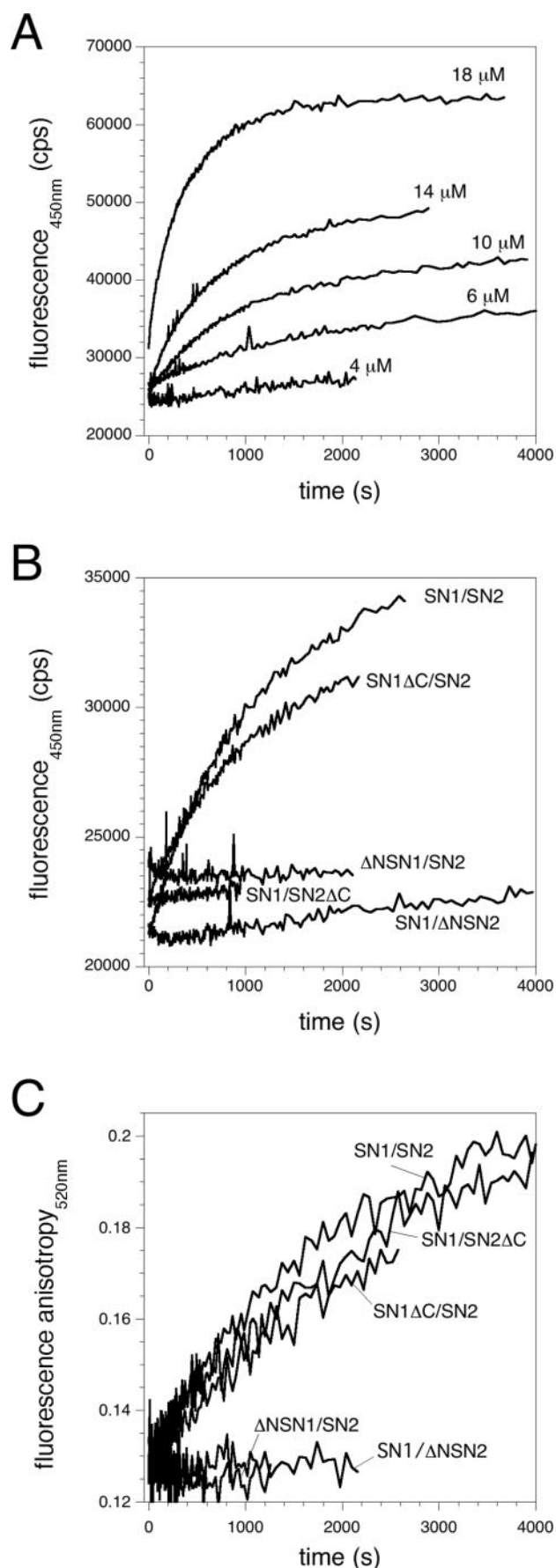


**FIG. 7. The N-terminal regions of both SNAP-25 helices cooperate during assembly.** A, SyxH3<sup>225IAANS</sup> (~200 nM) was mixed with increasing amounts of both individual helices of SNAP-25, SN1 (residues 1–83) and SN2 (residues 120–206). B, different combinations of

serve as a high affinity binding site for Snc1p (synaptobrevin homologue) (22). In line with these findings, it might be possible that the synaptic 1:1 Syx-SNAP-25 complex also consists of a three-helix bundle. *In vitro*, however, syntaxin has a tendency to occupy the fourth helix position, thereby obstructing the binding of synaptobrevin. However, it is unlikely that this “autoinhibitory” effect of syntaxin observed in the cuvette plays a major role *in vivo*. The majority of the abundant synaptic Q-SNAREs syntaxin and SNAP-25 appear to exist in distinct locations in the plasma membrane (25), suggesting that their interaction is tightly controlled. Nevertheless, the autoinhibitory effect of syntaxin on SNARE-mediated liposome fusion needs to be considered more critically, since it is likely that the Q-SNAREs in the membrane will also reside mainly as a 2:1 complex (4).

Truncation experiments showed that assembly of syntaxin and SNAP-25 requires the coordinated interaction of the Q<sub>a</sub> (Syntaxin), Q<sub>b</sub> (first helix of SNAP-25), and Q<sub>c</sub> helices (second helix of SNAP-25). Nucleation into a productive “Q<sub>abc</sub>” intermediate appears to be a prerequisite for subsequent synaptobrevin binding. Remarkably, only the N-terminal and not the C-terminal truncations of the Q-SNARE helices abolished nucleation. As discussed above, the structured region of the transient 1:1 Syx-SNAP-25 complex, in analogy to the Sso1p-Sec9p complex, might be restricted to its N-terminal portion. Obviously, perturbations in the N-terminal region would critically disturb this Q<sub>abc</sub> intermediate and thus render the energetic barrier for nucleation essentially insurmountable. Thus, at first glance, our data strongly support the idea that assembly of the Q<sub>abc</sub> intermediate starts with the contact of the N-terminal tips of the Q-SNARE motifs and proceeds in a zipper-like fashion toward the C-terminal membrane anchor region. However, it is also possible that the first contact is not restricted to the N-terminal tips but requires the entire N-terminal region of the participating Q-SNARE helices.

Interestingly, neither N- nor C-terminal truncations of synaptobrevin appeared to impair SNARE assembly. However, as discussed above, our approach did not allow us to directly analyze binding of synaptobrevin, which occurred after the formation of the Q<sub>abc</sub> intermediate. Thus, in principal, binding of synaptobrevin onto the Q<sub>abc</sub> intermediate could start from either direction. Interestingly, it was shown that synaptobrevin reconstituted into liposomes is inhibited from forming a SNARE complex, although its N-terminal portion appears to be free (26). This suggests a model in which binding of synaptobrevin starts with the C-terminal portion. However, it still seems more plausible that *in vivo* the free N terminus of synaptobrevin binds to the structured N-terminal portion of the Q-SNARE intermediate. Otherwise, to allow for a C-terminal start of assembly, the two membranes, assuming the zipper model is correct, would have to be pulled together by a so far unknown mechanism. Such a process would require energy that is actually thought to be produced by SNARE assembly.

In this study, we have focused on the soluble portions of the synaptic SNARE proteins. Thus, clearly, in the future, similar experiments need to be carried out in the presence of mem-

~10  $\mu$ M concentrations of the truncated variants of both individual SNAP-25 helices were added to SyxH3<sup>225IAANS</sup>. The following constructs were used:  $\Delta$ NSN1 (residues 39–83), SN1 $\Delta$ C (residues 7–66),  $\Delta$ NSN2 (residues 159–206), and SN1 $\Delta$ C (residues 141–188). C, the change in anisotropy of SyxH3<sup>225OG</sup> (~100 nM) in the presence of 10  $\mu$ M Syb was monitored over time upon mixing with 10  $\mu$ M concentrations of truncated variants of both individual SNAP-25 helices (see above). In these experiments, a somewhat shorter SN2 helix of SNAP-25 was used (SN2short; residues 141–204), which comprised the entire SNARE helix but lacked the turn of the helix-connecting linker region. However, no difference to the longer SN2 (residues 120–206) was observed.

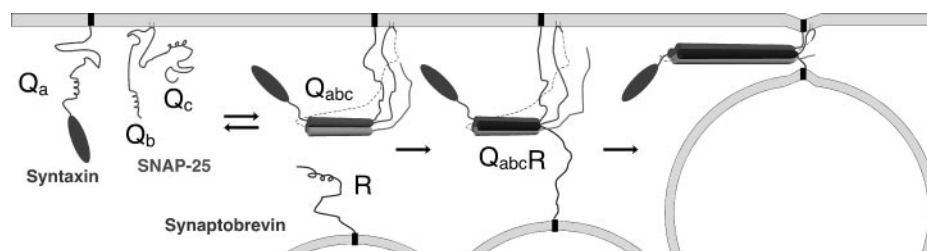


FIG. 8. **Schematic model of the sequence of SNARE assembly between synaptic vesicle and plasma membrane.** The two Q-SNAREs syntaxin and SNAP-25 reside in the plasma membrane, whereas the R-SNARE synaptobrevin is located in the membrane of neurotransmitter-loaded synaptic vesicles. For simplicity, the role of the N-terminal domain of syntaxin, which can slow down the Q-SNARE interaction, was neglected. In a rate-limiting nucleation step, the two Q-SNAREs form a complex, which involves the N-terminal region of all three Q-SNARE helices. It is likely that this nucleation step is controlled by accessory proteins. After establishment of the  $Q_{abc}$  intermediate, synaptobrevin can bind, forming a high affinity complex that shows little dissociation. It is unclear so far whether an additional assembly step takes place that involves a partially assembled trans-SNARE complex before final zippering and membrane fusion.

branes. Although the membrane fusion activity of SNAREs has been studied in some detail (17), so far knowledge of their activity and structure in membranes is rather sparse. Nevertheless, we believe that it is unlikely that the presence of the C-terminal transmembrane region will dramatically alter the properties of the distant soluble portion (see Ref. 4 for a more extended discussion).

Given the relatively simple four-helix bundle structure, it had been previously unclear why SNARE complex formation is slow. Our findings suggest that the slow rate can be explained by a structurally complex, and possibly unique, assembly mechanism. For productive assembly, the N-terminal portions of all three Q-SNARE helices have to come together in a parallel orientation. Two of these helices are part of one protein, SNAP-25, in which they are connected by a long flexible linker. Partition of the two helices caused the reaction to be much slower. The merger of two helices into one protein might therefore have offered a kinetic advantage for the process of synaptic exocytosis. In several other SNARE complexes that exist *in vivo*, however, the two helices are provided by two independent SNARE proteins. For these assembly processes, establishment of a  $Q_{abc}$  intermediate appears to be more challenging. On the other hand, the need to bring together three proteins to form an acceptor complex on one membrane may allow for a stricter control of the reaction. However, we cannot exclude the possibility that these SNAREs might utilize a somewhat different assembly pathway.

*In vivo*, Q-SNARE nucleation might be catalyzed by “priming” factors, which would help to arrange the Q-SNARE helices and stabilize the intermediate, rendering it available for vesicular R-SNARE binding. It is possible that the intricate assembly intermediate permits the tight control of the upcoming fusion process. It may also confer an element of Q-SNARE selectivity during the nucleation process.

Altogether, our data suggest that synaptic SNARE assembly starts with a rather complicated interaction of the N-terminal regions of all three Q-SNARE helices (Fig. 8). It is possible that only the structured N-terminal portion of this intermediate serves as high affinity binding site for a flexible synaptobrevin. Such a scenario would increase the capture radius of the proteins interacting between two still separated membranes. The relative instability of the  $Q_{abc}$  intermediate would provide a means of withholding and tightly controlling the upcoming, nearly irreversible, interaction with the cognate R-SNARE. It is unclear whether synaptobrevin binding occurs in a single

step or whether it proceeds through a stage in which only its N-terminal region is tightly bound. Such a partially assembled trans-complex might become stalled by an interaction with late acting factors, which eventually trigger complete assembly and thus neurotransmitter release upon the influx of  $Ca^{2+}$ .

**Acknowledgments**—We are greatly indebted to Matthias Böddener for excellent help in purifying proteins and protein complexes and Maria Druminski for plasmid construction. We thank Anand Radakrishnan, Frederique Varoqueaux, Matthew Holt, and Reinhard Jahn for critical reading of the paper.

#### REFERENCES

- Chen, Y. A., and Scheller, R. H. (2001) *Nat. Rev. Mol. Cell Biol.* **2**, 98–106
- Rizo, J., and Sudhof, T. C. (2002) *Nat. Rev. Neurosci.* **3**, 641–653
- Jahn, R., Lang, T., and Sudhof, T. C. (2003) *Cell* **112**, 519–533
- Fasshauer, D. (2003) *Biochim. Biophys. Acta* **1641**, 87–97
- Ungar, D., and Hughson, F. M. (2003) *Annu. Rev. Cell Dev. Biol.* **19**, 493–517
- Fasshauer, D., Bruns, D., Shen, B., Jahn, R., and Brünger, A. T. (1997) *J. Biol. Chem.* **272**, 4582–4590
- Fasshauer, D., Otto, H., Eliason, W. K., Jahn, R., and Brünger, A. T. (1997) *J. Biol. Chem.* **272**, 28036–28041
- Fasshauer, D., Eliason, W. K., Brünger, A. T., and Jahn, R. (1998) *Biochemistry* **37**, 10354–10362
- Hazzard, J., Sudhof, T. C., and Rizo, J. (1999) *J. Biomol. NMR* **14**, 203–207
- Margittai, M., Fasshauer, D., Pabst, S., Jahn, R., and Langen, R. (2001) *J. Biol. Chem.* **276**, 13169–13177
- Sutton, R. B., Fasshauer, D., Jahn, R., and Brünger, A. T. (1998) *Nature* **395**, 347–353
- Fasshauer, D., Sutton, R. B., Brünger, A. T., and Jahn, R. (1998) *Proc. Natl. Acad. Sci. U. S. A.* **95**, 15781–15786
- Bock, J. B., Matern, H. T., Peden, A. A., and Scheller, R. H. (2001) *Nature* **409**, 839–841
- Antonin, W., Fasshauer, D., Becker, S., Jahn, R., and Schneider, T. R. (2002) *Nat. Struct. Biol.* **9**, 107–111
- Hanson, P. I., Heuser, J. E., and Jahn, R. (1997) *Curr. Opin. Neurobiol.* **7**, 310–315
- Hay, J. C., and Scheller, R. H. (1997) *Curr. Opin. Cell Biol.* **9**, 505–512
- Weber, T., Zemelman, B. V., McNew, J. A., Westermann, B., Gmachl, M., Parlati, F., Sollner, T. H., and Rothman, J. E. (1998) *Cell* **92**, 759–772
- Xiao, W., Poirier, M. A., Bennett, M. K., and Shin, Y. K. (2001) *Nat. Struct. Biol.* **8**, 308–311
- Zhang, F., Chen, Y., Kweon, D. H., Kim, C. S., and Shin, Y. K. (2002) *J. Biol. Chem.* **277**, 24294–24298
- Rice, L. M., Brennwald, P., and Brünger, A. T. (1997) *FEBS Lett.* **415**, 49–55
- Nicholson, K. L., Munson, M., Miller, R. B., Filip, T. J., Fairman, R., and Hughson, F. M. (1998) *Nat. Struct. Biol.* **5**, 793–802
- Fiebig, K. M., Rice, L. M., Pollock, E., and Brünger, A. T. (1999) *Nat. Struct. Biol.* **6**, 117–123
- Fasshauer, D., Antonin, W., Subramaniam, V., and Jahn, R. (2002) *Nat. Struct. Biol.* **9**, 144–151
- Misura, K. M., Gonzalez, L. C., Jr., May, A. P., Scheller, R. H., and Weis, W. I. (2001) *J. Biol. Chem.* **276**, 41301–41309
- Lang, T., Bruns, D., Wenzel, D., Riedel, D., Holroyd, P., Thiele, C., and Jahn, R. (2001) *EMBO J.* **20**, 2202–2213
- Kweon, D. H., Kim, C. S., and Shin, Y. K. (2003) *Nat. Struct. Biol.* **10**, 417–419
- Fasshauer, D., Antonin, W., Margittai, M., Pabst, S., and Jahn, R. (1999) *J. Biol. Chem.* **274**, 15440–15446